Suggested Modifications for Bifacial Capacity Testing

Preprint

Martin Waters,[1] Chris Deline,[2] Johan Kemnitz,[1] and Jeffrey Webber[1]

1 Cypress Creek Renewables
2 National Renewable Energy Laboratory

Presented at the 46th IEEE Photovoltaic Specialists Conference (PVSC 46)
Chicago, Illinois
June 16-21, 2019

NREL is a national laboratory of the U.S. Department of Energy
Office of Energy Efficiency & Renewable Energy
Operated by the Alliance for Sustainable Energy, LLC

This report is available at no cost from the National Renewable Energy Laboratory (NREL) at www.nrel.gov/publications.

Contract No. DE-AC36-08GO28308

Conference Paper
NREL/CP-5K00-73982
October 2019

Suggested Modifications for Bifacial Capacity Testing

Preprint

Martin Waters,[1] Chris Deline,[2] Johan Kemnitz,[1] and Jeffrey Webber[1]

1 Cypress Creek Renewables
2 National Renewable Energy Laboratory

Presented at the 46th IEEE Photovoltaic Specialists Conference (PVSC 46)
Chicago, Illinois
June 16-21, 2019

Suggested Citation
Waters, Martin, Chris Deline, Johan Kemnitz, and Jeffrey Webber. 2019. *Suggested Modifications for Bifacial Capacity Testing: Preprint*. Golden, CO: National Renewable Energy Laboratory. NREL/ CP-5K00-73982. https://www.nrel.gov/docs/fy20osti/73982.pdf.

NREL is a national laboratory of the U.S. Department of Energy
Office of Energy Efficiency & Renewable Energy
Operated by the Alliance for Sustainable Energy, LLC

This report is available at no cost from the National Renewable Energy Laboratory (NREL) at www.nrel.gov/publications.

Contract No. DE-AC36-08GO28308

Conference Paper
NREL/CP-5K00-73982
October 2019

National Renewable Energy Laboratory
15013 Denver West Parkway
Golden, CO 80401
303-275-3000 • www.nrel.gov

Suggested Modifications for Bifacial Capacity Testing

Martin Waters,[1] Chris Deline,[2] Johan Kemnitz,[1] Jeffrey Webber[1]

[1] Cypress Creek Renewables, Santa Monica, CA 90405 USA; [2] National Renewable Energy Laboratory, Golden, CO 80401 USA

Abstract — **Capacity tests such as those described in ASTM 2848 and IEC 61724-2 are widely used during the contracting and acceptance testing of photovoltaic systems. With the increasing deployment of bifacial photovoltaic modules, there is a need to develop a standardized approach to capacity test these systems. Although variability and bias error were inherently higher for the measured capacity of bifacial systems, they could be reduced to a level consistent with the monofacial reference system by appropriate incorporation of rear irradiance—either measured or modeled. Three field installations provided bifacial system capacity that was measured with a mean bias error and standard deviation within 1% over the 2–10-month observation period. Capacity test accuracy could be improved further by using the measured back-of-module temperature and the IEC 61724-2 test method for well curated systems.**

I. Introduction

Capacity testing is widely used as a commercial acceptance mechanism for photovoltaic (PV) systems. It is valued in commercial settings for both its industry-wide acceptance and the relative speed at which these tests can be performed. Capacity tests are often used to demonstrate to project stakeholders that a PV system performs within expectations and that those test results can be tied to financial payments and milestones. However, the existing protocols do not specifically address the testing of systems using bifacial modules; nor do they account for the increased bifacial energy gain relative to front-side irradiance.

Bifacial modules are rapidly being adopted into the design and construction of PV systems, thus creating the need for contractual acceptance tests for these systems. This paper proposes a methodology for adapting the capacity testing methodology of ASTM 2848-13 [1] and will help inform draft revisions to IEC 61724-2 [2] to meet this need.

An input critical to capacity testing is the ability to measure the incident irradiance on the PV system. Based on preliminary deployments and system designs, we expect two variations in metrology that will need to be accounted for: 1) systems with a direct measurement of the rear-side plane-of-array (POA) irradiance (E_{Rear}), and 2) systems that do not have a direct measurement of E_{Rear}. Our examination of each of these configurations consists of a proposed modification to the existing standard, a validation with modeled data, and a validation against field measurements.

II. Capacity Test Methodology

The intent of a capacity test is to quickly compare actual performance of PV systems under ambient conditions against expected performance under pre-determined reporting conditions (RCs). The methods employed here begin by identifying a target period of performance (1-2 weeks) and filtering for abnormal (shade, snow) or cloudy conditions. Temperature and irradiance reporting conditions are chosen based on historical averages or observed conditions for the site.

The ASTM 2848-13 test employs a multiple linear regression of AC power (*P*) to E_{POA}, ambient temperature (T_a), and wind speed (v) through the following equation:

$$P = E_{POA}(a_1 + a_2 * E_{POA} + a_3 * T_a + a_4 * v). \quad (1)$$

Linear coefficients (a_1 through a_4) are identified for the period of performance and are used in conjunction with Eq. 1 to interpolate the system's *P* at target RCs. A comparison of P / P_{target} is accomplished by identifying system performance targets based on output of a system performance model.

The IEC 61724-2 test grew out of an intent to simplify the above method and to employ a deterministic rather than empirical temperature and irradiance correction [3]. In this approach, a correction factor (CF) based on temperature and irradiance is applied to measured power at each timestamp *i*:

$$P_{corr,i} = P_{meas,i} * CF_i\ , \quad (2)$$

where *CF* is based on the difference between measured conditions and RC:

$$CF = \left(\frac{E_{POA,RC}}{E_{POA}}\right)\left[1 + \delta\left(T_{cell} - T_{cell,RC}\right)\right]^{-1}, \quad (3)$$

where δ is the module temperature coefficient. Equations for cell temperature in the above equation are provided in Annex A of Ref. [2] based on measured T_a and wind speed, or back-of-module temperature. Both options are evaluated in this paper.

A. System Performance Target Model

Capacity test protocols often include a comparison of system performance against target expected performance. Bifacial PV systems behave in a similar fashion to monofacial PV systems with the added effect of converting rear-side irradiance into electricity. Bifacial performance models thus require characterization of the rear-side POA irradiance, which is typically based on either ray-tracing or view-factor mathematical models.

In this work, the National Renewable Energy Laboratory (NREL) created monthly system performance targets by using PVLib's 6-parameter model [4, 5] and measured current-voltage (IV) parameters of the modules [6]. The bifacial performance gain of the system was incorporated in the performance target by using actual measured E_{Rear} and Eq. (4). Cypress Creek Renewables (CCR) derived the system performance targets for each test period from a PVsyst model. This was done by applying Eq. 1— with the substitution of E_{total} for E_{POA} when E_{Rear} is considered—to the predicted system power from the PVsyst model and determining the linear regression coefficients. P_{target} was then found by substituting the parameters in Eq. 1 with the RCs derived from the observed meteorological conditions during each test period.

B. Modification of Capacity Method for Bifacial Systems

In the cases where a direct measurement of E_{Rear} is available, a simple modification to Eqs. (1) and (3) is made by substituting E_{Total} for E_{POA} to reflect the equivalent bifacial irradiance [7]:

$$E_{Total} = E_{POA} + E_{Rear} * \varphi \,, \qquad (4)$$

where E_{POA} is the measured front-side POA irradiance, E_{Rear} is the measured rear-side back-of-module irradiance, and φ is the specified bifaciality factor from the module spec sheet.

In the cases where the E_{Rear} is not measured directly, an alternate method is needed to determine the E_{Rear}. Due to the complex nature of deriving the E_{Rear}, we suggest using a readily available model. Ideally, the model allows for the inputs of the available measured data and the outputs of the modeled data at the same frequency as the measurements taken in the field. In addition, the model should not require any tools or proprietary methods that a party to a contractual capacity test might not be able to access.

For this paper, we used NREL's System Advisor Model (SAM), which recently implemented the Bifacial VF model [8]. In addition to implementing this model, SAM has the ability to process data down to a one-minute resolution and can include varying albedo measurements. Multiple components of irradiance (diffuse, global, direct) are required to generate accurate E_{Rear} values.

If the model that is used to set the contractual energy target (contractual model) differs from the model used to process the operational data (operational model), then the operational model parameters need to be adjusted such that the model produces an E_{Rear} within an acceptable level of precision relative to the contractual model under the same set of inputs. For example, if the contractual model is set using a software that only supports hourly outputs and the test requires higher fidelity data and thus a different software, the operational model should be tuned such that the desired output matches the contractual model when the same weather file is utilized in each model as seen in figure 2. The operational model predicted E_{Rear} derived from observed inputs can then be used in conjunction with Eq. 4 and with either Eq. 1 or 3 to run a capacity test on the system.

III. Model-Based Validation

A. Measured E_{Rear}

To validate the above methodology, the first step was to ensure that the regression derived from modeled data would produce results in line with the modeled expectations. To do this, a bifacial system was modeled using PVsyst software with varying albedo settings from 0.2 to 0.8, ensuring that the method is robust to varying albedo.

The modeled outputs were then filtered to remove low irradiance periods and points where the facility was clipping. This dataset was regressed using Eq. 1, with the substitution of E_{Total} for E_{POA}, to create a system-specific set of regression coefficients. Once these coefficients were determined, the relative meteorological inputs were fed into the regression to predict the power at each data point. The regression-derived power was then compared to the PVsyst-predicted power for each data point. The hourly residuals on power are seen in Fig. 1. The sum of the regression-derived power from all data points was 99.99% of the sum of PVsyst-predicted power, thus indicating that the regression is capable of matching the model-predicted behavior of the system.

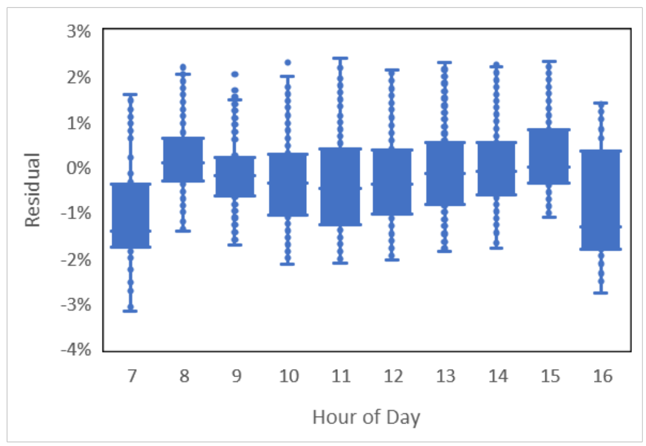

Fig. 1. Residuals by hour of the day for an annualized regression of the PVsyst-based model using the form of Eq. 1 with substitution of E_{Total}.

B. Model-Derived E_{Rear}

Modeled E_{Rear} can have significant variability depending on the model chosen (SAM vs PVsyst) and the meteorological inputs available (single E_{POA} vs direct normal irradiance [DNI] and diffuse horizontal irradiance [DHI]). The SAM operational model was run in its highest-accuracy mode given all three components of irradiance—global horizontal irradiance (GHI), DHI, and DNI—to calculate E_{Rear}. It was then run a second time, given only front-side E_{POA} from this initial model run. This replicates the operational scenario when only E_{POA} is available and not the more accurate DHI and DNI model inputs as seen in Fig. 2. Variability in E_{Rear} modeled from each operational model run was then examined. Relative to the combined E_{Total}, running SAM based on the lower accuracy E_{POA} input results in 0.5% error on average and up to 4.5% maximum due to the variation in the predicted E_{Rear}.

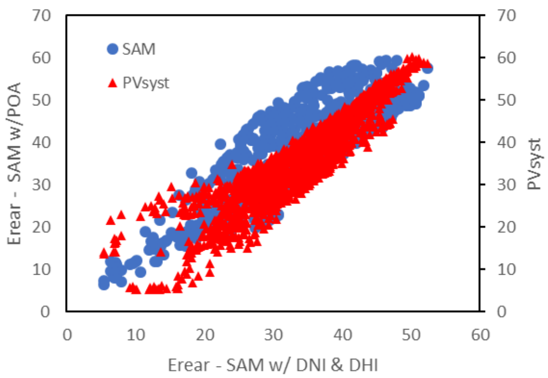

Fig. 2. SAM operational model run with two irradiance components (DNI and DHI) or only one (E_{POA}) results in varying E_{Rear} [W/m^2] predictions shown in blue. SAM operational model run with two irradiance components (DNI and DHI) compared to PVsyst contractual model.

IV. Field Validation

Three installations were used to validate the methods described above. The first is a small test installation (Fig. 3) deployed in Golden, CO, which consists of a 2.16-kW string of monofacial PERC modules and a string of 1.62-kW bifacial PERC modules. E_{POA} and E_{Rear} are measured with forward- and backward-facing reference cells. The system is south-oriented at a fixed tilt of 30 degrees with the modules mounted 2-in-portrait. Horizontal ground albedo is measured at the site with upward- and downward-facing reference cells.

Fig. 3. Field test installation consisting of bifacial and monofacial strings.

Data were collected for a period of a year. Due to naturally changing ground cover and the presence of snow in the winter, ground albedo is variable, with the highest variability in the month of February.

The second system is a small test facility located in Jackson, MI, which consists of multiple bifacial technologies and a monofacial reference. The system is mounted on the center row of a three-row single-axis tracker with modules mounted 2-in-portrait with a row of dummy modules on either side. Power measurements are made at the module level. E_{POA}, E_{Rear}, and GHI measurements are made with Secondary Standard thermopile pyranometers; DHI measurements are made with a SPN1 diffuse pyranometer; and albedo measurements are made with a second-class thermopile pyranometer-based albedometer.

The third system is a 1-MW facility located in Asheboro, NC, which consists of predominantly bifacial modules with a small monofacial reference array. The system is mounted on single-axis trackers with modules mounted 2-in-portrait. The system has 25-kW string inverters, which allows each inverter to be examined as an independent system. E_{POA}, E_{Rear}, and GHI measurements are made with Secondary Standard thermopile pyranometers; DHI measurements are made with a SPN1 diffuse pyranometer; and albedo measurements are made with a second-class thermopile pyranometer-based albedometer.

Data from each of the three test sites were run through a matrix of tests in Table 1. Each test is carried out for both the ASTM and IEC methodologies.

Table 1. Test matrix for examination of bifacial testing

System	Measured E_{POA}	Measured E_{Rear}	Modeled E_{Rear}
Monofacial	x		
Bifacial	x		
Bifacial	x	x	
Bifacial	x		x

Tests are run on a rolling basis: 7-day windows are sufficient for data collection in Golden, whereas the other two facilities require 14-day windows for sufficient data collection. Periods of stable irradiance are isolated using the statistical technique from section 9.1.7.1 of [1]. RCs are chosen based on prevailing environmental conditions during each period studied. Data are filtered to ensure unconstrained inverter operation, and median RCs were found for each test period. An example of raw and filtered data is seen in Fig. 4.

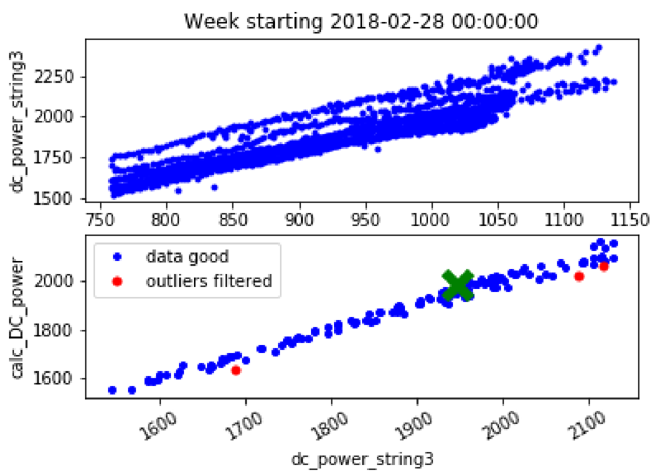

Fig. 4. Monofacial data (Golden, CO) showing DC power vs E_{POA} (top) and ASTM regressed field data vs measured data (bottom). Red points are rejected by a statistical outlier filter. Green cross indicates Pmeasured vs Ptarget at RC.

A. Monofacial Reference

Each site in the test has an associated monofacial reference array. The results of the monofacial tests are found in Table 2.

Table 2. Mean and standard deviation of monofacial reference tests

Site	Test Period	n	Test	μ	σ [%]
Golden, CO	9/1/2017–7/31/2018	316	ASTM	0.98	0.86
			IEC	0.98	0.72
Asheboro, NC	3/14/2019 –5/5/2019	39	ASTM	0.98	0.66
			IEC	0.98	0.72
Jackson, MI	2/20/2019 –5/6/2019	51	ASTM	1.02	0.60
			IEC	1.02	0.94

B. Bifacial with E_{POA}

Each bifacial system was tested using only the E_{POA} component of measured irradiance as the input into the test. The results of this test are found in Table 3.

Table 3. Mean and standard deviation for bifacial systems using only E_{POA}

Site	Test Period	n	Test	μ	σ [%]
Golden, CO	9/1/2017–7/31/2018	316	ASTM	1.01	0.87
			IEC	1.02	0.76
Asheboro, NC	3/14/2019 –5/5/2019	39	ASTM	1.02	0.61
			IEC	1.02	0.77
Jackson, MI	2/20/2019 –5/6/2019	51	ASTM	1.02	0.64
			IEC	1.02	0.64

C. Bifacial with E_{Total}

Each bifacial system was tested using the measured E_{Total} as the input into the test. The results of this test are found in Table 4.

Table 4. Mean and standard deviation for bifacial systems using E_{Total}

Site	Test Period	n	Test	μ	σ [%]
Golden, CO	9/1/2017–7/31/2018	316	ASTM	0.98	0.82
			IEC	0.99	0.77
Asheboro, NC	3/14/2019 –5/5/2019	39	ASTM	1.01	0.66
			IEC	1.01	0.47
Jackson, MI	2/20/2019 –5/6/2019	51	ASTM	1.00	0.57
			IEC	1.00	0.78

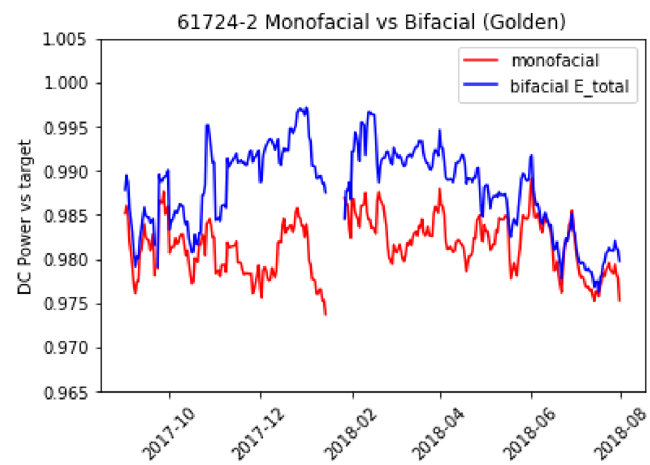

Fig. 5. Bifacial and monofacial test scores over a year-long period at Golden, CO, using measured E_{Total}.

D. Bifacial with E_{Total} Using Modeled E_{Rear}

Each bifacial system was tested using E_{Total}—comprising measured E_{POA} and modeled E_{Rear}—as the input into the test. E_{Rear} was derived from measured GHI, DHI, and albedo input into SAM. The results of this test are found in Table 5.

Table 5. Mean and standard deviations for bifacial systems using modeled E_{Rear} for a composite E_{Total}

Site	Test Period	n	Test	μ	σ [%]
Golden, CO	9/1/2017–7/31/2018	316	ASTM	0.98	0.90
			IEC	0.99	0.81
Asheboro, NC	3/14/2019 –5/5/2019	39	ASTM	1.03	0.60
			IEC	1.03	0.52
Jackson, MI	2/20/2019 –5/6/2019	51	ASTM	1.02	0.53
			IEC	1.02	0.71

E. IEC 61724-2 Model – Module Temperature

The IEC 61724-2 method was also evaluated at the Golden, CO, site for a comparison of measured back-of-module temperatures with measured T_a and wind speed for the monofacial system. The results of this test are found in Table 6.

Table 6. Mean and standard deviations for measured and derived back-of-module temperature

Site	System	Temperature measurement	μ	σ [%]
Golden, CO	Monofacial	Tmod	0.98	0.31
Golden, CO	Monofacial	T_a, Wind Speed	0.98	0.72

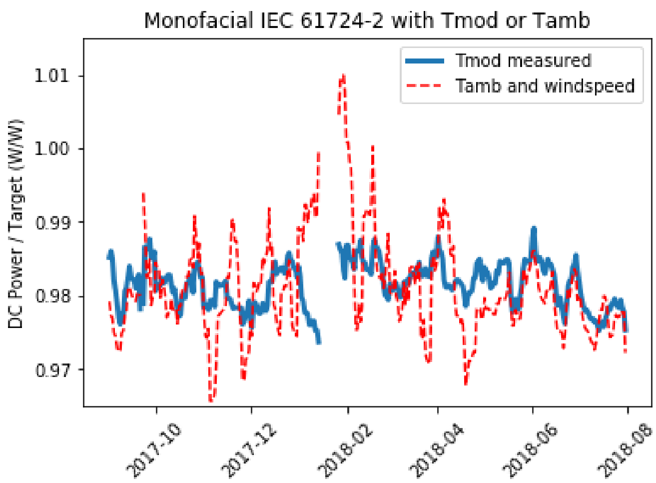

Fig. 6. IEC 61724-2 capacity test of monofacial system (Golden, CO) indicates substantial improvement in weekly standard deviation by using measured T_{mod} rather than modeled T_{mod} from T_a and v.

In some instances, incorrect T_{mod} measurements have resulted in substantial bias error, e.g., from detached thermocouples. However, for this well-curated system, using measured T_{mod} substantially improved the resulting standard deviation without introducing bias error as seen in Table 6 and Fig. 6.

VI. Findings

Initial model-based validation (Section III) indicated that the substitution of E_{Total} into the ASTM 2848 regression equation would adequately capture the behavior of bifacial systems. This finding was confirmed by field measurements in Section IV. Whether modeled or measured, the inclusion of E_{Rear} was found to improve the consistency of capacity testing results for bifacial systems for both the IEC and ASTM methods (Table 3 vs Table 4). This is particularly so for periods of time experiencing variable albedo (Fig. 7). When including E_{Rear} in the capacity test, results for bifacial systems can achieve comparable mean bias error and standard deviation to monofacial systems (Fig. 5, Table 2 vs Table 4).

When comparing modeled E_{Rear} vs measured E_{Rear}, the findings were mixed. For all three of the systems, modeled E_{Rear} showed a similar or lower σ variability in regressed power compared to measured E_{Rear}. However, the Asheboro, NC and Jackson, MI sites had a significant increase in the bias error by using modeled E_{Rear}. The increased bias error in particular could be caused by consistent under-prediction of E_{Rear} and bifacial gain by the bifacial model employed.

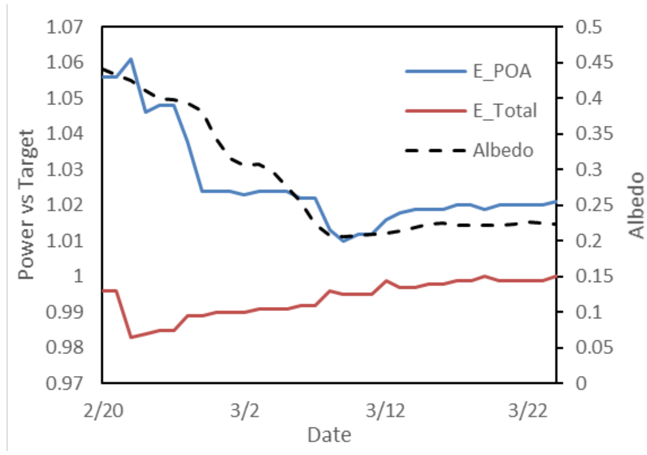

Fig. 7. Test dependence on albedo with and without the inclusion of E_{Rear}.

A. E_{Rear} Model Residuals

Further investigation into the differences between modeled and measured E_{Rear} is given here. For the fixed-tilt Golden, CO site, modeled E_{Rear} was found to match measurement with relatively small bias error. For the two single-axis tracking systems however, expected E_{Rear} derived from observed meteorological conditions and the SAM model was found to be consistently lower than measured E_{Rear} (Fig. 8). The upward bias in the mean of the test scores when using modeled E_{Rear} compared to measured E_{Rear} can be attributed in part to this error.

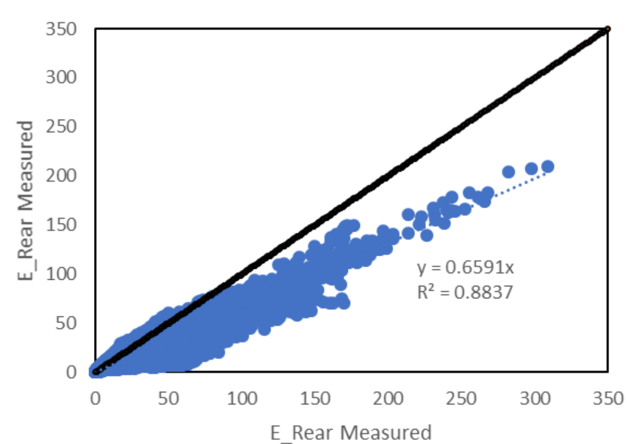

Fig. 8. Example of modeled and measured E_{Rear} at Jackson, MI with underprediction by the SAM model, typical of the two single axis tracker locations.

B. Temperature Effects in Capacity Testing

The analysis here has focused primarily on the use of E_{Rear}, but the proper treatment of temperature and temperature coefficient (δ_{Pmp}) can be equally important. The IEC 61724-2 procedure in particular is able to enjoy significant improvements in method stability by substituting directly measured T_{mod} as opposed to modeled from T_a and wind speed, as shown in Fig. 6 and Table 6.

The proper selection of δ_{Pmp}, both in Eq. (3) and for calculation of P_{target}, will also influence the stability and accuracy of the capacity test. In relative terms, uncertainty in E_{Rear} and albedo can be rather low on the list of contributors to overall system uncertainty. Based on Eq. (4), given a system with module bifaciality $\varphi = 0.75$ and E_{Rear} / E_{POA} = 8%, the following factors will have the same contribution to uncertainty as a hypothetical 20% E_{Rear} bias error: a 1.1% error in either E_{POA} or module P_{mp} rating, a 2.3°C error in T_{Mod}, or 0.00035 error in δ_{Pmp} (e.g., -0.00465 °C^{-1} rather than -0.0043 °C^{-1}). These are all relatively small values, so although E_{Rear} contributes to the calculation of bifacial system capacity, careful treatment of other performance parameters remains equally important.

Acknowledgements

This work was supported by the U.S. Department of Energy under Contract No. DE-AC36-08-GO28308 with the National Renewable Energy Laboratory (NREL). Funding provided by the U.S. Department of Energy's Office of Energy Efficiency and Renewable Energy (EERE) under Solar Energy Technologies Office (SETO) Agreement Number 34910.

This material is based upon work supported by the U.S. Department of Energy, Office of Science, Office of Energy Efficiency and Renewable Energy (EERE), Solar Energy Technologies Office under Award Number DE-EE0008564.

References

[1] ASTM E2848-13, "Standard Test Method for Reporting Photovoltaic Non-Concentrator System Performance," 2013.

[2] IEC TS 61724-2, "Photovoltaic System Performance – Part 2: Capacity Evaluation Method," October 2016.

[3] T. Dierauf, S. Kurtz, E. Riley, and B. Bourne, "A Fundamentals Approach to Plant Capacity Testing," *Proceedings of the 29th European Photovoltaic Solar Energy Conference and Exhibition (EU PVSEC 2014)*, September 22, 2014. https://www.osti.gov/biblio/1312470

[4] W. Holmgren, C. Hansen, and M. Mikofski, "pvlib python: A Python Package for Modeling Solar Energy Systems," *Journal of Open Source Software*, **3**(29), 884, 2018. https://doi.org/10.21105/joss.00884

[5] W. De Soto et al., "Improvement and Validation of a Model for Photovoltaic Array Performance," *Solar Energy*, **80**, 78–88, 2006.

[6] A. Dobos, "An Improved Coefficient Calculator for the California Energy Commission 6 Parameter Photovoltaic Module Model," *Journal of Solar Energy Engineering*, **134**, 2012.

[7] IEC TS 60904-1-2, "Photovoltaic Devices–Part 1-2: Measurement of Current-Voltage Characteristics of Bifacial Photovoltaic (PV) Devices," January 2019.

[8] B. Marion, S. MacAlpine, C. Deline, A. Asgharzadeh, F. Toor, D. Riley, J. Stein, and C. Hansen, "A practical irradiance model for bifacial PV modules," 44th IEEE Photovoltaic Specialists Conference, Washington, D.C., 2017.